Englander, S. W., & Wand, A. J. (1987) *Biochemistry 26*, 5953-5958.
Forst, S., Weiss, J., Elsbach, P., Maraganore, J. M., Reardon, I., & Heinrikson, R. L. (1986) *Biochemistry 25*, 8381-8385.
Hammond, S. J., Birdsall, B., Searle, M. S., Roberts, G. C. K., & Feeney, J. (1986) *J. Mol. Biol. 188*, 81-97.
Jansen, E. H. J. M. (1979) Ph.D. Thesis, Rijksuniversiteit te Utrecht, The Netherlands.
Jansen, E. H. J. M., Meyer, H., de Haas, G. H., & Kaptein, R. (1978) *J. Biol. Chem. 253*, 6346-6347.
Jansen, E. H. J. M., van Scharrenburg, G. J. M., Slotboom, A. J., de Haas, G. H., & Kaptein, R. (1979) *J. Am. Chem. Soc. 101*, 7397-7399.
Marion, D., & Wuthrich, K. (1983) *Biochem. Biophys. Res. Commun. 113*, 967-974.
Nieuwenhuizen, W., Kunze, H., & de Haas, G. H. (1974) *Methods Enzymol. 32B*, 147-154.
Okamoto, M., Ono, T., Tojo, H., & Yamano, T. (1985) *Biochem. Biophys. Res. Commun. 128*, 788-794.
Renetseder, R., Dijkstra, B. W., Huizinga, K., Kalk, K. H., & Drenth, J. (1988) *J. Mol. Biol. 200*, 181-188.
Slotboom, A. J., Jansen, E. H. J. M., de Haas, G. H., Vlijm, H., Pattus, F., & Soares de Araujo, P. (1978) *Biochemistry 17*, 4593-4600.
Van Wezel, F. M., & de Haas, G. H. (1975) *Biochim. Biophys. Acta 410*, 299-309.
Verheij, H. M., Slotboom, A. J., & de Haas, G. H. (1981) *Rev. Physiol. Biochem. Pharmacol. 91*, 91-203.
Waite, M. (1987) *Handbook of Lipid Research*, Vol. 5, Plenum Press, New York.
Weber, P. L., Drobny, G., & Reid, B. R. (1985a) *Biochemistry 24*, 4549-4552.
Weber, P. L., Wemmer, D. E., & Reid, B. R. (1985b) *Biochemistry 24*, 4553-4562.
Wuthrich, K. (1986) in *NMR of Proteins and Nucleic Acids*, Wiley, New York.

^{1}H NMR Studies of Porcine Calbindin D_{9k} in Solution: Sequential Resonance Assignment, Secondary Structure, and Global Fold†

Torbjörn Drakenberg,‡,§ Theo Hofmann,‖ and Walter J. Chazin*,‡

Department of Molecular Biology, Research Institute of Scripps Clinic, 10666 North Torrey Pines Road, La Jolla, California 92037, and Department of Biochemistry, University of Toronto, Toronto, Ontario M5S 1A8, Canada

Received January 19, 1989; Revised Manuscript Received March 31, 1989

ABSTRACT: The ^{1}H nuclear magnetic resonance (NMR) spectrum of Ca^{2+}-saturated porcine calbindin D_{9k} (78 amino acids, M_r 8800) has been assigned. Greater than 98% of the ^{1}H resonances, including spin systems for each amino acid residue, have been identified by using an approach that integrates data from a wide range of two-dimensional scalar correlated NMR experiments [Chazin, Rance, & Wright (1988) *J. Mol. Biol. 202*, 603-626]. Due to the limited quantity of sample and conformational heterogeneity of the protein, two-dimensional nuclear Overhauser effect (NOE) experiments also played an essential role in the identification of spin systems. On the basis of the pattern of scalar connectivities, 43 of the 78 spin systems could be directly assigned to the appropriate residue type. This provided an ample basis for obtaining the sequence-specific resonance assignments. The elements of secondary structure are identified from sequential and medium-range NOEs, values of $^3J_{NH\alpha}$, and the location of slowly exchanging backbone amide protons. Four well-defined helices and a mini β-sheet between the two calcium binding loops are present in solution. These elements of secondary structure and a few key long-range NOEs provided sufficient information to define the global fold of the protein in solution. Generally good agreement is found between the crystal structure of the minor A form of bovine calbindin D_{9k} and the solution structure of intact porcine calbindin D_{9k}. The only significant difference is a short one-turn helix in the loop between helices II and III in the bovine crystal structure, which is clearly absent in the porcine solution structure.

Calbindin D_{9k} (formerly intestinal calcium binding protein) is a small, acidic, and very heat stable protein found in the small intestine of all mammalian species so far examined (Kallfelz et al., 1967; Drescher & De Luca, 1971; Hitchman & Harrison, 1972; Taylor, 1983). It belongs to the troponin C superfamily of calcium regulatory proteins that are characterized by a common helix-loop-helix motif for the calcium binding sites, termed EF-hands (Kretsinger, 1972). These proteins exhibit changes in conformation in response to binding of metal ions, the presumed structural basis for function. While the synthesis of calbindin D_{9k} has been shown to be vitamin D dependent (Corradino et al., 1976), its function is not well understood. It is agreed that the protein is involved in Ca^{2+} ion transport (Wasserman et al., 1983) or as a Ca^{2+} reservoir or buffer (Mayel-Afsharet, 1988). The X-ray crystal structure of the minor A form of the bovine calbindin D_{9k} has been refined to 2.3-Å resolution (Szebenyi & Moffat, 1986). Recently, the gene encoding for the bovine protein has been synthesized and expressed in *Escherichia coli* (Brodin et al., 1986), allowing for study by protein engineering and biophysical methods (Linse et al., 1987, 1988; Wendt et al., 1988; Forsén et al., 1988).

† This work was supported by grants from the National Institutes of Health (GM40120 to W.J.C.) and the Swedish Natural Sciences Research Council (T.D.).
* To whom correspondence should be addressed.
‡ Research Institute of Scripps Clinic.
§ Permanent address: Division of Physical Chemistry II, Chemical Center, University of Lund, P.O. Box 124, S-221 00 Lund, Sweden.
‖ University of Toronto.

0006-2960/89/0428-5946$01.50/0

As part of our concerted efforts to determine the structural basis for function of this class of calcium regulatory proteins, we are using ^{1}H NMR[1] spectroscopy to examine conformation in solution. Here we report on a study of the solution structure of porcine calbindin D_{9k} in the Ca^{2+}-loaded form. The porcine protein is one residue longer than the bovine protein, but is expected to have a very similar conformation because there is over 90% amino acid sequence homology[2] between the two (Hofmann et al., 1979; Fullmer & Wasserman, 1981). Unless special precautions are taken, some of the N-terminal amino acid residues will be cleaved off during purification, leaving the minor A (75 amino acids) or minor B (74 amino acids) forms (Fullmer & Wasserman, 1973). In contrast to the crystallographic studies, our studies have been carried out on the intact protein. For convenience in making comparisons, the numbering scheme based on recombinant minor A calbindin D_{9k} (Brodin et al., 1986) has been adopted; thus, the N-terminal serine in intact porcine calbindin D_{9k} is number −2, etc.

In this paper the spin system analysis and sequence-specific assignment of the ^{1}H NMR spectrum of Ca^{2+}-loaded porcine calbindin D_{9k} are presented. In addition, the complete assignments provide the necessary background for analyzing the pattern of NOE connectivities, scalar coupling constants, and backbone amide proton exchange rates to determine the elements of regular secondary structure and establish the nature of the global fold. These structural features are then compared to those observed in the crystal structure of the minor A form of bovine calbindin D_{9k}.

Materials and Methods

The protein was purified as reported previously (Hitchman et al., 1973). A single 8-mg sample was used for all experiments. The sample was dissolved in H_2O/5% ^2H_2O, giving a 2 mM protein solution, and the pH was adjusted to 6.0. For convenience this will be referred to as H_2O solution. A series of spectra were acquired from this solution, and then the sample was lyophilized and redissolved in ^2H_2O, and a spectrum was recorded starting 2 h after dissolution. The solution was then heated to 65 °C for 2 h, lyophilized, and dissolved in "100%" ^2H_2O (MSD Isotopes).

All ^{1}H NMR experiments were carried out on Bruker AM 500 spectrometers equipped with Aspect 3000 computers and digital phase shifting hardware. 2D NMR spectra were recorded and processed as described in detail in Chazin et al. (1988b). NOESY spectra were acquired with a Hahn echo period added after the observe pulse (M. Rance, unpublished experiments) to improve the quality of the base line [see Davis (1989)]. The following spectra were acquired from the H_2O solution at 300 K: COSY; R-COSY with τ = 38 ms; DR-COSY with τ_1 = 22 ms and τ_2 = 40 ms; TOCSY with spin lock periods of 60 and 100 ms; 2Q with τ = 30 ms; Hahn echo NOESY with τ_m = 40, 80, and 200 ms. To obtain unambiguous assignment data for backbone amide proton resonances that are degenerate at 300 K, one additional COSY and NOESY data set was acquired at 315 K. A Hahn echo NOESY spectrum with τ_m = 200 ms was recorded by using the sample prepared with protein lyophilized from ^1H_2O and dissolved in ^2H_2O. This spectrum provided the qualitative backbone amide proton exchange data for Figure 5. The following 2D spectra were acquired from the ^2H_2O solution: 2QF-COSY; 2Q with τ = 30 ms; 3QF-COSY; 3Q with τ = 22 ms; TOCSY with spin lock periods of 57, 70, and 103 ms; Hahn echo NOESY with τ_m = 200 ms.

Results

Spin System Identification. ^{1}H spin systems of Ca^{2+}-loaded porcine calbindin D_{9k} were identified by using the general assignment strategy described in Chazin et al. (1988b). The bulk of the analysis is made from a series of spectra acquired in H_2O solution that provide relayed connectivities from the amino acid side-chain protons to the corresponding backbone amide proton. The advantages of this approach have been described previously (Chazin & Wright, 1987). This analysis is supplemented by searching for relayed connectivities to the ^{1}H resonances of the amino acid side-chain termini (e.g., leucine $C^\delta H_3$, lysine $C^\epsilon H_2$). Matching of the spin subsystems based at the backbone and side-chain termini provide the complete assignments for those spin systems that cannot be identified solely from relayed connectivities to the backbone amide proton. Multiple quantum and multiple quantum filtered COSY spectra are then utilized to confirm these assignments and unambiguously distinguish between the various protons of each side chain. The goal of this strategy is to classify all spin systems as unique (glycine, alanine, threonine, valine, leucine, isoleucine, arginine, and lysine), 3-spin or 5-spin based on the characteristic patterns of proton scalar connectivities. This primary classification is subsequently refined by utilizing characteristic NOEs from asparagine and glutamine side-chain amide protons or from aromatic ring protons to the corresponding backbone, C^β or C^γ protons, to provide residue-specific assignments for spin systems initially classified as 3-spin or 5-spin. These extensive spin system and residue type assignments then provide an ample basis for obtaining sequence-specific assignments by using the sequential resonance assignment procedure (Billeter et al., 1982).

In this particular instance the spin system identification steps have not been pushed to the extreme due to the complications introduced by the existence of two isomers in the native folded protein (Chazin et al., 1989) and by the limited quantity of protein available. As a result, when a sufficiently large set of residue-specific assignments had been obtained (about 60% of the amino acid residues), the sequential resonance assignment procedure was started, even though not all scalar coupling information was analyzed at this point. The complete assignments for all residues were obtained by iterating through the scalar correlated and NOESY spectra. The proline spin systems were identified only after nearly all other spin systems were sequentially assigned. Every effort was made to unambiguously differentiate the spin systems of the major (75%) conformational isomer. We are confident of the correctness of our analysis because a self-consistent set of essentially complete resonance assignments has been obtained (Table I).

(*A*) *Preliminary Analysis.* The characteristic backbone fingerprint region ($\omega_1 \sim$ 6.0–3.0 ppm, $\omega_2 \sim$ 10.5–6.5 ppm) of the COSY spectrum of porcine calbindin D_{9k} should contain cross peaks for 74 residues (78 residues minus the four prolines; the N-terminal serine is acetylated and gives rise to a cross peak). At pH 6.0 and 300 K cross peaks from far more than 74 residues appear in the spectrum (Figure 1). In all, 96

[1] Abbreviations: NMR, nuclear magnetic resonance; 1D, one-dimensional; 2D, two-dimensional; COSY, correlation spectroscopy; R-COSY, relayed COSY; DR-COSY, double-relayed COSY; 2Q (3Q), two quantum (three quantum) spectroscopy; 2QF-COSY (3QF-COSY), two quantum filtered (three quantum filtered) COSY; TOCSY, total correlation spectroscopy; NOE, nuclear Overhauser enhancement; NOESY, 2D NOE spectroscopy; 3-spin, the $C^\alpha H$–$C^\beta H_2$ spin system of serine, aspartic acid, asparagine, and the aromatic amino acid residues; 5-spin, the $C^\alpha H$–$C^\beta H_2$–$C^\gamma H_2$ spin system of methionine, glutamic acid, and glutamine residues.

[2] The residue at position 58 was reported as asparagine in Hofmann et al. (1979), but was subsequently identified as aspartic acid (T.H., unpublished experiments).

Table I: ^{1}H NMR Chemical Shifts of Ca^{2+}-Loaded Porcine Calbindin D_{9k} (pH 6.0, 300 K)[a]

residue	chemical shifts (ppm)					
	NH	C^α	C^β	C^γ	C^δ	other
S −2	8.31	4.43	3.83, 3.87			
A −1	8.45	4.38	1.41			
Q 00	8.28	4.36	1.98, 2.09	2.37, 2.37		[c]
K 01	8.50	4.57	1.79, 1.79	1.56, 1.56[b]	1.71, 1.71	2.99, 2.99 (C^ϵ)
S 02	9.09	4.78	4.06, 4.39			
P 03	–	4.34	2.49, 1.99	2.24, 2.07	3.98, 3.93	
A 04	8.22	4.16	1.43			
E 05	7.99	4.14	2.41, 2.07	2.31, 2.43		
L 06	8.59	4.25	2.19, 1.71	1.90	1.05, 0.98	
K 07	8.24	3.97	1.94, 1.76	0.80, 1.19	1.29, 1.34	2.57, 2.63 (C^ϵ)
S 08	7.85	4.28	4.01, 4.01			
I 09	8.23	3.83	2.17	2.00, 1.19	0.94	1.14 ($C^\gamma H_3$)
F 10	8.41	3.54	2.71, 3.33			6.35, 7.11, 7.615 (C^δ, C^ϵ, C^ζ)
E 11	8.55	3.75	2.11, 1.94	2.68, 2.33		
K 12	7.75	3.82	1.75, 1.80	0.48, 1.10	1.41, 1.45	2.68, 2.68 (C^ϵ)
Y 13	7.22	3.98	2.42, 2.80			7.39, 6.73 (C^δ, C^ϵ)
A 14	8.36	3.78	0.42			
A 15	6.91	4.30	1.42			
K 16	7.17	3.85	2.17, 1.90	1.47, 1.47[b]	1.71, 1.76	2.75, 2.91 (C^ϵ)
E 17	9.70	4.72	1.88, 2.00	2.22, 1.92		
G 18	9.01	3.64, 3.97				
D 19	8.32	4.68	2.63, 2.86			
P 20	–	4.80	2.22, 2.02	2.07, 1.87	3.98, 3.98[b]	
N 21	9.01	4.96	2.70, 3.02			6.96, 7.94 ($N^\gamma H_2$)
Q 22	7.23	5.11	1.83, 2.01	2.11, 2.26		6.58, 7.46 ($N^\delta H_2$)
L 23	9.55	5.48	2.07, 1.55	1.28	0.73, 0.34	
S 24	10.09	4.81	4.35, 4.18			
K 25	8.71	3.45	1.29, 0.45	0.98, 0.65	1.33, 1.38	2.56, 2.57 (C^ϵ)
E 26	7.98	4.01	1.83, 2.00	2.37, 2.14		
E 27	7.73	3.90	1.86, 2.34	1.89, 2.28		
L 28	8.82	4.06	1.59, 2.23	1.77	1.12, 1.08	
K 29	8.41	3.61	1.85, 2.09	1.18, 1.33	1.63, 1.63	2.82, 2.82 (C^ϵ)
Q 30	7.79	3.87	2.18, 2.00	2.69, 2.43		7.69, 6.79 ($N^\delta H_2$)
L 31	8.02	2.33	1.71, 1.18	1.27	0.92, 0.80	
I 32	8.83	3.46	1.90	1.77, 1.22	0.75	0.89 ($C^\gamma H_3$)
Q 33	8.38	3.78	2.10, 1.95	2.53, 2.32		7.17, 6.80 ($N^\delta H_2$)
A 34	7.44	4.27	1.54			
E 35	8.21	4.33	1.32, 1.31	2.12, 2.48		
F 36	8.38	5.25	2.73, 3.36			7.135, 7.135, 6.98 (C^δ, C^ϵ, C^ζ)
P 37	–	4.12	2.45, 1.23	1.95, 1.90	3.13, 3.51	
S 38	8.40	4.18	3.90, 3.98			
L 39	8.06	4.13	1.86, 1.48	1.77	0.75, 0.79	
L 40	7.40	4.44	1.74, 1.70	1.55	0.95, 0.79	
K 41	7.35	4.47	1.73, 1.97	1.40, 1.57	1.65, 1.65	2.96, 2.96 (C^ϵ)
G 42	8.04	4.22, 4.12				
P 43	–	4.42	2.26, 2.03	2.04, 1.94	3.74, 3.57	
R 44	7.99	4.64	1.92, 1.77	1.65, 1.65	3.15, 3.17	7.49
T 45	8.36	4.28	4.48	1.38		
L 46	8.82	3.99	1.72, 1.83	1.66	0.94, 0.94[b]	
D 47	8.03	4.22	2.68, 2.55			
D 48	7.89	4.35	2.88, 2.68			
L 49	8.39	4.13	1.76, 1.70	1.60	0.81, 0.80	
F 50	8.98	3.64	2.99, 3.22			7.1–7.2 (C^δ, C^ϵ, C^ζ)
Q 51	7.84	3.97	2.21, 2.17	2.46, 2.56		[c]
E 52	7.67	3.88	2.06, 1.88	2.26, 1.97		
L 53	7.93	4.14	1.14, 1.64	2.00	0.82, 0.73	
D 54	7.93	4.55	2.48, 1.57			
K 55	8.05	4.04	1.86, 1.85	1.69, 1.50	1.74, 1.73	3.09, 3.05 (C^ϵ)
N 56	7.92	4.81	3.29, 2.85			6.63, 8.04 ($N^\gamma H_2$)
G 57	7.58	3.83, 3.80				
D 58	8.22	4.63	3.13, 2.46			
G 59	10.48	4.28, 3.70				
E 60	7.77	5.13	1.44, 1.90	2.18, 2.00		
V 61	10.38	5.12	2.34	1.24, 0.51		
S 62	9.55	4.88	4.22, 4.53			
F 63	9.61	3.32	2.43, 2.65			6.49, 7.125, 7.35 (C^δ, C^ϵ, C^ζ)
E 64	8.47	3.86	2.05, 1.89	2.25, 2.33		
E 65	7.98	4.07	2.56, 2.38	2.60, 2.60[b]		
F 66	8.91	3.97	3.14, 3.30			6.91, 7.20, 7.14 (C^δ, C^ϵ, C^ζ)
Q 67	7.60	3.44	1.89, 1.95	2.30, 2.12		5.77, 6.15 ($N^\delta H_2$)
V 68	7.07	3.54	1.96	1.01, 0.81		
L 69	7.15	3.72	1.32, 1.25	1.21	0.69, 0.48	
V 70	6.84	3.15	1.97	0.74, 0.60		
K 71	7.44	4.00	1.75, 1.83	1.38, 1.45	1.58, 1.58	2.88, 2.88 (C^ϵ)
K 72	7.48	4.12	1.83, 1.83	1.35, 1.47	1.42, 1.58	2.69, 2.81 (C^ϵ)
I 73	7.41	4.07	1.84	1.22, 0.83	0.29	0.64 ($C^\gamma H_3$)
S 74	7.69	4.51	3.85, 3.85			
Q 75	7.70	4.14	1.93, 2.09	2.30, 2.30[b]		[c]

[a] Chemical shifts are referenced to the H_2O signal at 4.75 ppm and are accurate to ±0.02 ppm, except for strongly coupled pairs of protons (separated by <0.1 ppm), where accuracy is ±0.03 ppm. These assignments are for the major (*trans*-Pro43) form of the protein. [b] Degeneracy of the protons is inferred. [c] Side-chain NH_2 resonances could not be assigned due to lack of NOE cross peaks.

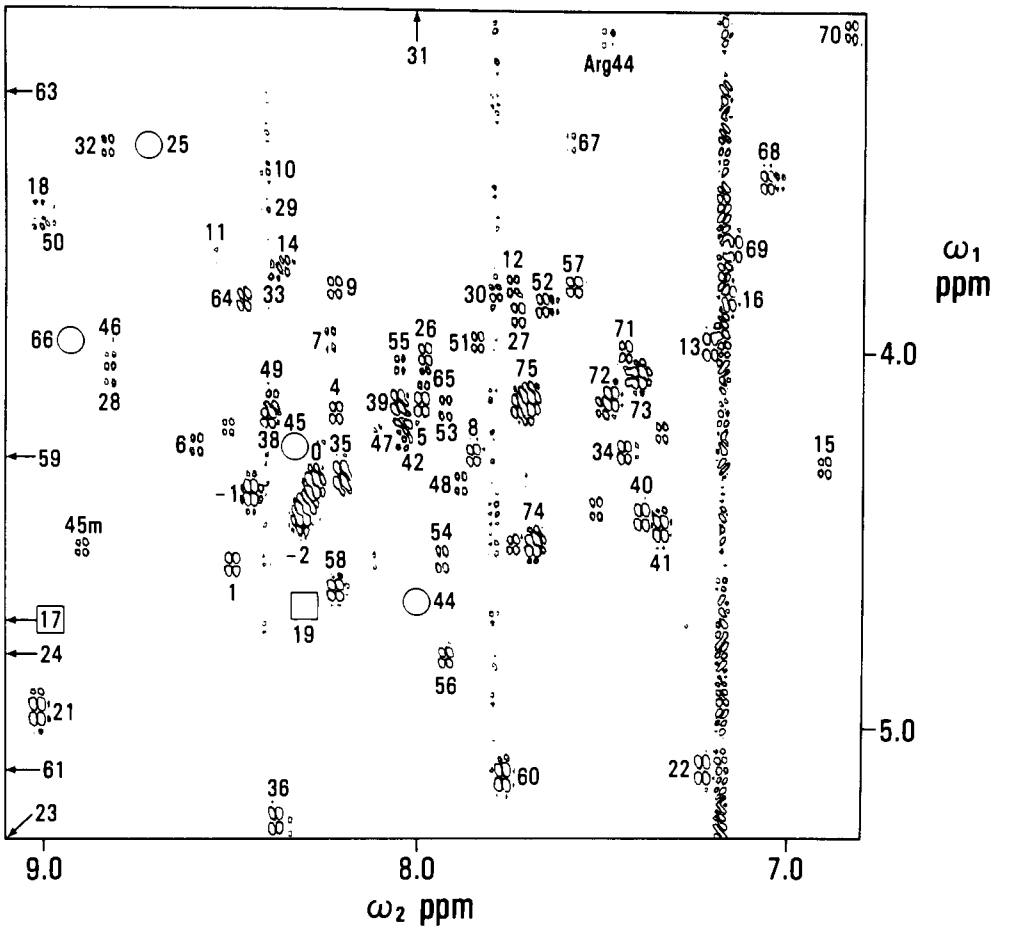

FIGURE 1: Backbone fingerprint region from a 500-MHz COSY spectrum of a 2 mM solution of Ca^{2+}-loaded porcine calbindin D_{9k} at pH 6.0 and 300 K. The ω_1 = $C^{\alpha}H$, ω_2 = NH cross peaks are labeled with the sequence-specific assignment. Arrows indicate cross peaks that appear outside the region shown. Boxes show the location of cross peaks not observed in this spectrum, but which could be identified in other 2D spectra. Circles are drawn around cross peaks that can only be observed at very low contour levels. The peak marked 45m is from the minor isomer of Thr45. Several other minor isomer cross peaks are clearly evident, but are not specifically identified.

discrete cross peaks were identified. This overabundance is due to cis–trans isomerism at Pro43 as discussed in a previous paper (Chazin et al., 1989). Even though the cis form of Pro43 is present at the level of only 25%, the relative intensities of the backbone NH/$C^{\alpha}H$ cross peaks in the COSY spectrum cannot be used to distinguish between resonances from the major and minor forms because the intensity of a COSY cross peak depends strongly on the active spin coupling. In fact, due to significant differences in backbone conformation, a few cross peaks from the less abundant cis form are more intense than the corresponding cross peaks from the more abundant trans form. A clear-cut example is identified in Figure 1. For Thr45, $^3J_{HN\alpha}$ is very small in the major (trans) isomer and the corresponding COSY cross peak is greatly attenuated (only observed at low contour levels). In contrast, the cross peak for the minor (cis) isomer is clearly observed, despite the fact that it is present at only one-third concentration, because $^3J_{HN\alpha}$ is much larger. A more reliable estimate of relative abundance could be obtained by comparing corresponding cross peaks in TOCSY and NOESY spectra.

In the characteristic region of the COSY spectrum containing the alanine $C^{\alpha}H/C^{\beta}H_3$ and threonine $C^{\beta}H/C^{\gamma}H_3$ cross peaks, five strong cross peaks, one somewhat weaker cross peak, and several very weak cross peaks are readily identified for the five alanine residues and the single threonine. In the valine/leucine/isoleucine fingerprint region, 27 of the 29 methyl doublet resonances expected for the 3 valine, 10 leucine, and 3 isoleucine residues could be identified in a straightforward manner. The absence of two of the cross peaks is due to accidental degeneracy of $C^{\delta}H_3$ and $C^{\delta'}H_3$ resonances of Leu46 (0.91 ppm) and of Leu49 (0.80 ppm). In addition to these strong cross peaks several low-intensity cross peaks are observed in this region. Since scalar coupling to methyl groups does not vary significantly, the low-intensity signals can without exception be assigned to resonances of the minor form. Two of the three pairs of anti-phase triplet cross peaks for the three isoleucine C^{δ} methyl groups are readily identified. For the third isoleucine (Ile32) only one of the $C^{\gamma}H/C^{\delta}H_3$ cross peaks is readily apparent; the other was subsequently found to overlap with the $C^{\gamma}H/C^{\delta}H_3$ cross peaks of Leu39.

The ring protons of the tyrosine and three of the five phenylalanines could be identified in a straightforward manner. A resonance at 6.35 ppm from one of the remaining phenylalanine rings was significantly broadened at 300 K and therefore did not show any cross peaks in the COSY spectrum. The cross peak to this resonance could be observed in the spectrum recorded at 315 K. For the fifth phenylalanine no cross peaks could be observed in any of the 2D spectra due to degeneracy of all five resonances. This assignment was based on the integration of the aromatic region in a 1D spectrum acquired from a ^2H_2O solution with all labile protons exchanged. Surprisingly, there is no sign of resonance doubling due to the cis–trans isomerism in the aromatic region.

(B) Identification of Spin Systems. The identification of the spin systems corresponding to many of the 96 backbone cross peaks identified in the COSY spectrum was made from the series of COSY, 2Q, R-COSY, DR-COSY, and TOCSY spectra acquired from ^1H_2O solution. The attribution of spin

systems to the minor form was facilitated in many cases by the observation of two very similar sets of relayed connectivities from the corresponding side-chain protons, one set of significantly lower intensity than the other.

Two of the four glycine spin systems were identified from their characteristic multiplet structure in the COSY spectrum. These assignments were confirmed, and the three other glycine spin systems (one for the minor isomer) were identified from the observation of remote cross peaks at $\omega_2 = \omega_{NH}$ and $\omega_1 = \omega_\alpha + \omega_{\alpha'}$ in the 2Q spectrum acquired from a ^1H_2O solution. The complete spin systems of the five alanines were identified in the R-COSY spectrum. The single threonine and three valine spin systems could be completely identified in the DR-COSY spectrum.

The three backbone amide based isoleucine spin subsystems were identified by $C^\gamma H_3$/NH cross peaks in the DR-COSY spectrum. However, relayed connectivities from each of the side-chain resonances to the NH resonance were observed only for Ile73. The complete spin systems of Leu40, Leu49, and Leu69 were also identified from relayed connectivities in the ^1H_2O spectra. The other isoleucine and leucine spin systems could be assigned by matching the corresponding side-chain resonances that were identified via relayed connectivities, to both the backbone NH and the $C^\gamma H_3$ or $C^\delta H_3$ resonances. For Ile9, Ile32, Leu31, and Leu39, the complete set of side-chain resonances could only be identified from analysis of MQ, MQF-COSY, and TOCSY spectra acquired in ^2H_2O. The assignment of each of the side-chain resonances was subsequently verified in the 2Q spectrum acquired in ^2H_2O.

Seventeen of the 20 3-spin spin systems were identified in straightforward manner via relayed connectivities to the backbone amide proton. These assignments were verified in MQ and MQF-COSY spectra. Although relayed connectivities were not observed for the three other spin systems (Asp19, Ser24, and Ser62), the C^β protons could be identified by $C^\alpha H/C^\beta H$ connectivities in MQ and MQF-COSY spectra. The three $C^\alpha H$ chemical shifts were distinctive enough so that the identity of the corresponding backbone amide proton could be obtained directly from the $C^\alpha H$/NH cross peaks in the COSY spectrum. The tyrosine, five phenylalanine, and two asparagine spin systems could be assigned through the observation of cross peaks between the C^β protons and either the aromatic protons or the side-chain amide protons in NOESY spectra. The seven serines were specifically identified on the basis of $C^\beta H$ chemical shifts >3.8 ppm. A resonance at 5.98 ppm exhibited NOESY cross peaks to the backbone amide and C^β protons of Ser62 and to the C^β protons of Glu65 and is assigned to the $O^\gamma H$ of Ser62. Since no other Ser $O^\gamma H$ resonances are observed under these experimental conditions, we assume that exchange with solvent for this resonance is reduced by strong hydrogen bonding, presumably to Glu65 as observed in the crystal structure (Szebenyi & Moffat, 1986).

Eleven of the 17 5-spin spin systems were identified in the amide-based analysis through observation of both C^β proton resonances and at least one C^γ proton resonance with a chemical shift greater than 2.0 ppm. The remaining assignments were obtained from MQF-COSY, MQ, and TOCSY spectra in ^2H_2O. For both Glu65 and Gln75, only one resonance could be identified for the C^γ protons, and degeneracy was therefore assumed. Four of the 5-spin spin systems could be assigned to glutamines through the observation of NOESY cross peaks between the C^γ protons and side-chain amide protons. The remaining three glutamines (Gln0, Gln51, and Gln75) could only be distinguished after the sequence-specific assignment.

The spin system for the single arginine could be identified by the coincidence of relayed connectivities in the backbone amide and C^δ proton based spin subsystems. The side-chain NH proton signal was identified by the $C^\delta H_2$/NH cross peak in the amide region of the COSY spectrum. The strategy used to completely identify the lysine spin systems is described in detail in Chazin et al. (1987). Seven of the 10 lysine spin systems could be completely identified on the basis of a unique combination of relayed connectivities to both the backbone NH and $C^\epsilon H_2$ resonances. The three other lysines were identified in a similar manner, except that the unique combinations of relayed connectivities were observed at the $C^\alpha H$ and $C^\epsilon H_2$ resonances. Since only one resonance was observed in all 2D spectra for the $C^\gamma H_2$ of Lys1 and Lys16, these were assumed to be degenerate. In all other instances, the degeneracy of lysine side-chain proton resonances was firmly established by remote peaks in 2Q and/or by direct and remote peaks in 3Q spectra.

(*C*) *Identification of Proline Spin Systems.* Identification of the four proline spin systems was deferred until the final stages of spin system analysis. Unassigned resonances in the $C^\alpha H$ region of the 2QF-COSY, 2Q, 3QF-COSY, and 3Q spectra (ω_2 = 3–5 ppm) were tentatively assigned as C^α and C^δ proton resonances from the prolines. This resulted in four C^α–$C^\beta H_2$ and two $C^\gamma H_2$–$C^\delta H_2$ fragments. By use of the same strategy as for the lysine residues, the coincidence of the relayed connectivities to both $C^\alpha H$ and $C^\delta H_2$ resonances provided complete assignments for two spin systems, subsequently identified as Pro37 and Pro43. The assignments for Pro3 and Pro20 were obtained only after the preceding and following residues were assigned in a squence-specific manner. For these two prolines the two halves of the spin system could not be connected in any of the scalar correlated experiments. However, in both cases the sequential resonance assignments leading to and from the residue are unambiguous, and intraresidue NOESY cross peaks could be detected between the corresponding $C^\alpha H$ and $C^\delta H_2$ resonances.

Sequence-Specific Assignment. The sequential resonance assignments were made by using data from NOESY spectra acquired with a mixing time of 200 ms. Cross peaks for interproton distances up to 4.5 Å are detectable and may include a limited contribution from spin diffusion, as verified by comparison to the spectra obtained with 40- and 80-ms mixing times. The shorthand notation of Wüthrich et al. (1984) for specifying short proton–proton distances and corresponding NOE connectivities has been followed. Figure 2 shows traces of consecutive $d_{NN}(i, i + 1)$ NOE connectivities that provide sequence-specific assignments for four major segments of the protein sequence. Nearly all of the remaining sequence-specific assignments were obtained through the observation of strong $d_{\alpha N}(i, i + 1)$ connectivities. A summary of the results of applying the sequential resonance assignment procedure (Billeter et al., 1982) to Ca^{2+}-loaded porcine calbindin D_{9k} is shown in Figure 3. At this stage it was also possible to clearly distinguish a number of cross peaks in the NOESY spectra between resonances of the minor isomer. The assignments in the minor species have not been pursued in the present work, since a complete analysis has been carried out on the highly homologous bovine protein (Chazin et al., 1989; Kördel et al., 1989).

Secondary Structure. Helical regions can be identified on the basis of a network of consecutive $d_{NN}(i, i + 1)$ NOE connectivities, medium-range [$(i, i + 2)$, $(i, i + 3)$, and $(i, i + 4)$] NOE connectivities, small scalar coupling constants ($^3J_{HN\alpha}$), and slow amide proton exchange. These data for

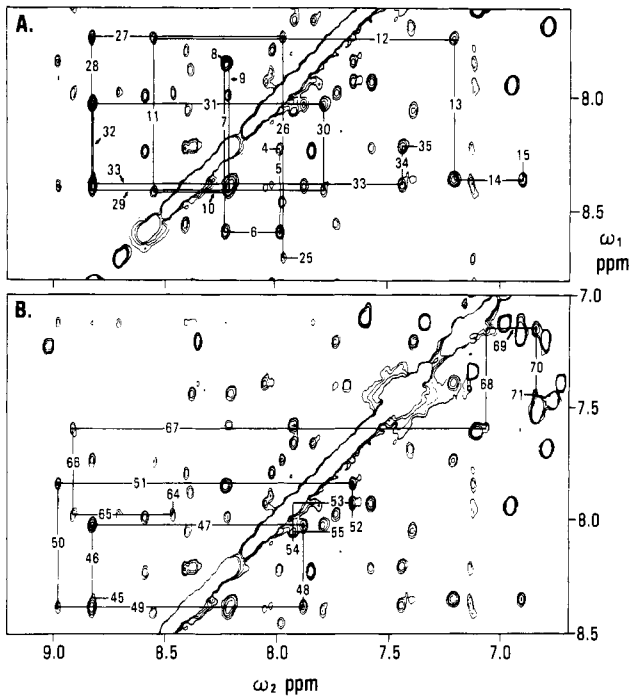

FIGURE 2: Sequential resonance assignments for polypeptide segments in helical conformation. Regions from a 500-MHz Hahn echo NOESY spectrum (τ_m = 200 ms) of a 2 mM solution of Ca^{2+}-loaded porcine calbindin D_{9k} at pH 6.0 and 300 K show d_{NN} connectivities. Lines are drawn between pairs of $d_{NN}(i, i-1)$ and $d_{NN}(i, i+1)$ cross peaks and labeled with the sequence-specific assignments. The experimental data are shown for a portion of helix I (Ala4–Ala15) and most of helix II (Lys25–Glu35) in (A) and for all of helix III (Thr45–Asp54) and a portion of helix IV (Glu64–Lys71) in (B).

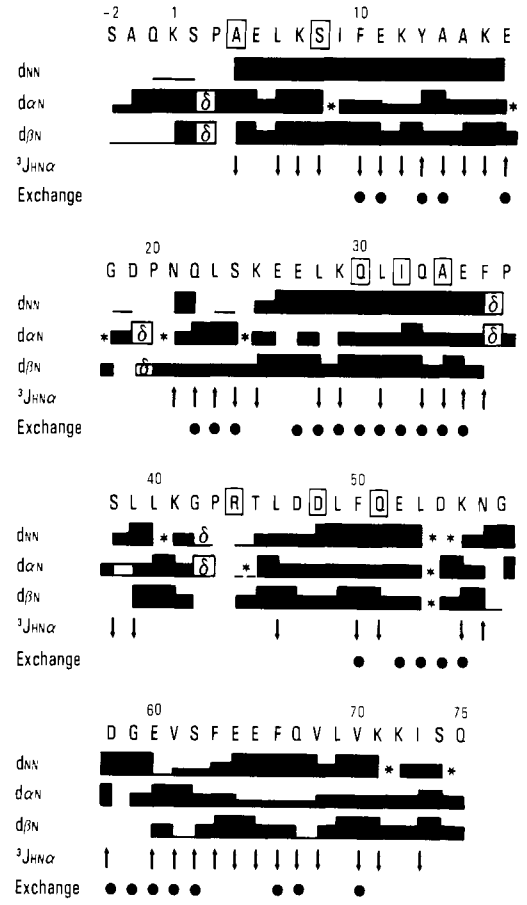

FIGURE 3: Summary of sequential NOE connectivities, backbone spin coupling constants ($^3J_{HN\alpha}$), and slow amide proton exchange rates observed in solution for Ca^{2+}-loaded porcine calbindin D_{9k}. The one-letter codes for the amino acids are given at the top. Boxes denote sequence differences with respect to the bovine protein. Characteristic NOE connectivities [$d_{NN}(i, i+1)$, $d_{\alpha N}(i, i+1)$, $d_{\beta N}(i, i+1)$] are indicated by lines or bars between the two residues. The height of the bars gives a qualitative measure of the relative strength of the NOE in the 200-ms NOESY spectrum. Connectivities that could not be identified due to degeneracy of resonances or due to saturation are labeled with an asterisk (*). Connectivities to proline $C^\delta H_2$ resonances are marked with a delta (δ). Values of $^3J_{HN\alpha}$ are classified as small (<6 Hz) and large (>8 Hz) as indicated by ↓ and ↑, respectively. Backbone amide protons that exchange slowly are indicated with a dot (●).

porcine calbindin D_{9k} are summarized in Figures 3 and 4. The location of helices on the basis of the above criteria is indicated in Figure 4, along with the helical segments in the X-ray crystal structure. We have assigned helical structures for the polypeptide segments Ser2–Lys16, Ser24–Glu35, Thr45–Asp54, and Ser62–Ser74, designated helices I, II, III, and IV, respectively. We note varying degrees of fraying at both ends of each helix, as indicated in Figure 4.

The observation of large spin coupling constants ($^3J_{NH\alpha}$ > 8 Hz) together with strong sequential $d_{\alpha N}$ NOE connectivities indicates two short stretches of extended backbone conformation for residues 22–24 and 60–62. Furthermore, the NOESY spectrum shows NOEs between protons in these two segments. These data indicate a β-sheet-type interaction as depicted in Figure 5.

Using the previously defined criteria (Wüthrich et al., 1984; Wagner et al., 1986), we find that in the second Ca^{2+} ion binding loop NMR evidence is present for a type I turn from Asp54 to Gly57 which would, in effect, correspond to an extra distorted/frayed turn of helix III. A second tight turn in this Ca^{2+} binding loop is implicated for the polypeptide segment Asp56–Gly59; however, the inability to determine the backbone dihedral angles for residue 2 (Gly57) of the turn because stereospecific assignments of glycine residue have not been made precludes a definite assignment. This putative tight turn would be interwoven with the preceding turn from Asp54 to Gly57 and could also be interpreted as a further extension of helix III.

Global Fold. Using the elements of regular secondary structure and some key NOEs between protons from residues well separated in the sequence, it is possible to schematically diagram the tertiary structure of Ca^{2+}-loaded porcine calbindin D_{9k}. In the following, we describe the global fold by specifying the contacts and constraints between the various elements of secondary structure, building up from the N-terminus.

Extending from helix I (Ser2–Lys16), the polypeptide segment Glu17–Pro20 is constrained to loop back toward the helix, since a very close contact with Ala15 is found (strong NOE between the C^α protons of Ala15 and Pro20). This segment continues on to the short β-strand (Gln22–Ser24) and back again, constrained by a strong NOE between Leu23 and Ala14. This contact also establishes that the C-terminus of helix I is close to the N-terminus of helix II. The helices must be packed in an antiparallel fashion, as indicated by the NOEs between Tyr13 and Ile9 of helix I and Leu31, Ala34, and Glu35 of helix II. The sequence from Glu35 to Thr44 is less well defined from the presently identified tertiary NOEs; however, it is constrained to loop around to meet the N-terminus of helix III. The position of helix III (Thr45–Asp54) is well-defined with respect to helix II by strong NOEs observed between the side chain of Leu28 and the C^α proton of Phe50 and between the side chain of Leu46 and the C^α proton of Lys29. Helix III is therefore packed antiparallel to helix II. The absence of contacts between helices I and III positions them on opposite sides of helix II. The relative disposition of

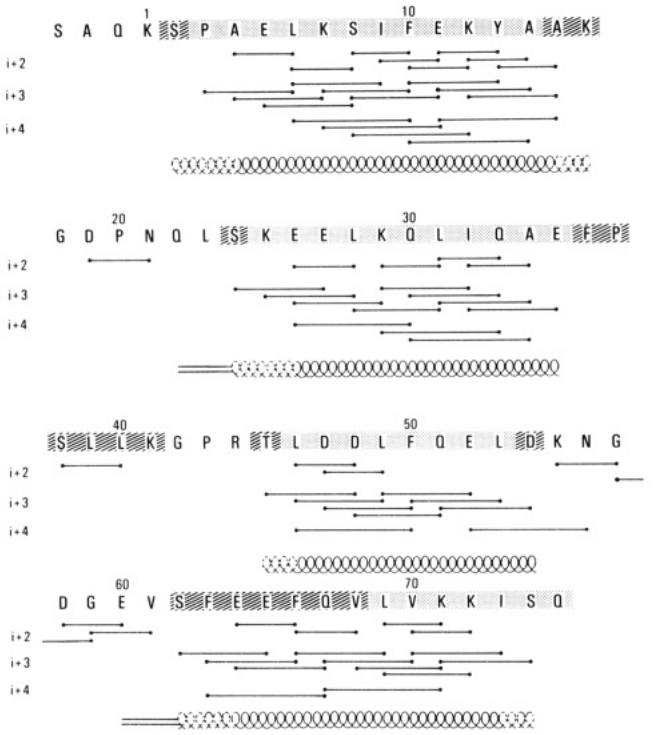

FIGURE 4: Summary of medium-range NOE connectivities that aid in the identification of the helical segments of Ca^{2+}-loaded porcine calbindin D_{9k} in solution. The one-letter codes for the amino acid residues in the sequence are given at the top. The locations of helices in the crystal structure are indicated by shading for "good" α-helices and by crosshatching for other helical regions (Szebenyi & Moffat, 1986). Characteristic NOE connectivities [$d_{\alpha N}(i, i + 2)$, $d_{\alpha N}(i, i + 3)$, $d_{\alpha\beta}(i, i + 3)$, $d_{\alpha N}(i, i + 4)$] are indicated by lines between the two connected residues. The location of elements of secondary structure in solution is indicated by coils for helices and by solid lines for the β-sheet. Distorted helical segments and helix fraying are indicated by coils drawn with dashed lines.

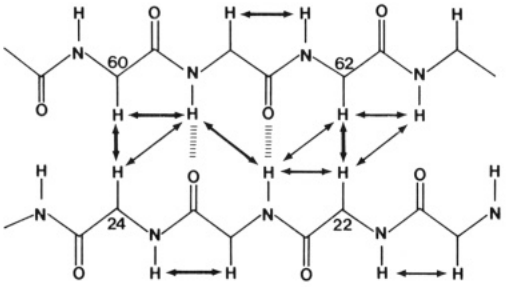

FIGURE 5: Diagram of the short β-sheet identified in Ca^{2+}-loaded porcine calbindin D_{9k} showing the observed NOE connectivities (double-headed arrows). The width of the arrows give a qualitative measure of the relative strength of the NOE connectivities in the 200-ms NOESY spectrum. The hydrogen bonds that can be assigned on the basis of NMR data are shown by crosshatched vertical bars.

the second Ca^{2+} binding loop is constrained by the antiparallel β-interaction with the first Ca^{2+} binding loop. The loop must therefore extend back toward the helix I/helix II interface. The N-terminus of helix IV is positioned by NOEs between Leu53 and Val61 as well as between Leu53 and Phe66. Finally, the fourth helix (Ser62–Ser74) can be positioned relative to the other helices through NOEs observed between Ile73 and Leu6 in helix I and between Val70 and Ile32 in helix II. Helix IV is parallel to helix II and antiparallel to helices I and III.

Schematic diagrams of the folding topology are shown in Figure 6. In summary, we find that the four helices of the protein form a small bundle, with the two Ca^{2+} binding loops extending out from the same end of the bundle and held in close contact by the hydrogen bonds of the mini β-sheet.

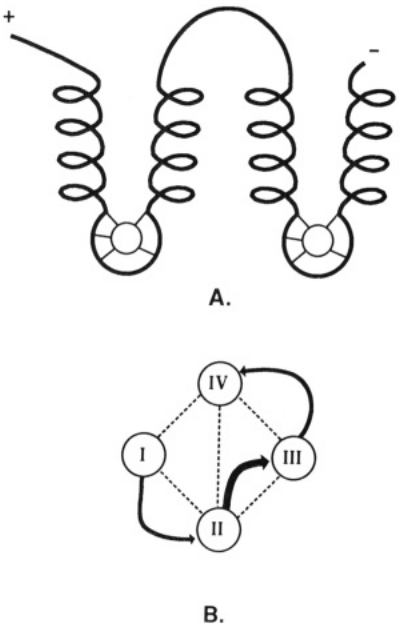

FIGURE 6: Schematic diagrams of the global fold of Ca^{2+}-loaded porcine calbindin D_{9k} in solution. (A) Two-dimensional diagram of the chain-folding topology. Helices are represented by coils. The Ca^{2+} binding loops fold around circles representing the Ca^{2+} ions. (B) Two-dimensional representation of topology and packing of the four helices. The curved thick line represents loops above and the curved thin lines represent loops below the body of the helical bundle. The dashed lines indicate the helix/helix contacts that are identified by NOEs and serve to establish the relative packing of the helices.

Discussion

The sequence-specific assignment of the ^1H NMR spectrum of Ca^{2+}-loaded porcine calbindin D_{9k} has been completed for all 78 amino acid residues. The only remaining uncertainties are for 12 nonproven degeneracies in some lysines, glutamines, and glutamic acid residues and the identity of the side-chain amides of Gln0, Gln51, and Gln75. We stress that this has all been achieved by using a single 8-mg sample of the protein. These results and corresponding studies of the bovine protein (Chazin et al., 1989; Kördel et al., 1989) provide the first complete ^1H NMR assignment of proteins in the troponin C superfamily of calcium binding proteins. There are several discrepancies with respect to assignments based on a limited set of 1D NMR experiments on minor A bovine calbindin D_{9k} (Dalgarno et al., 1983).

For the prototypical EF-hand Ca^{2+} binding loop II of porcine calbindin D_{9k} [and the highly homologous bovine calbindin D_{9k} (Kördel et al., 1989)], the glycine at the sixth position of the loop has a uniquely low field shifted NH resonance, as observed in calmodulin (Ikura et al., 1987), in the two C-terminal sites of rabbit skeletal troponin C (Tsuda et al., 1988), and in pike parvalbumin (Padilla et al., 1988). In addition, we note that C^α chemical shifts are greater than 4.75 ppm for the seventh and eighth residues. These unique chemical shifts are the result of the corresponding residues being involved in a β-sheet-type interaction. For the N-terminal Ca^{2+} binding site in bovine and porcine calbindin D_{9k}, the glycine in the sixth position is replaced by two residues, proline and asparagine, and we observe that only Ser24 at position 11 has a backbone NH shift greater than 10 ppm. Interestingly, the residues in positions 7–11 (Pro20–Ser24) do have $C^\alpha H$ chemical shifts greater than 4.75 ppm. On the basis of these results, it appears that *regular* EF-hand calcium binding sites (in the calcium-loaded form) are distinguished by the combination of chemical shifts >10 ppm for the

backbone amide proton of the residue at position 6 and >4.75 ppm for the C^α protons of the residues in positions 7 and 8.

Generally, there is an excellent agreement between the secondary structural elements reported by Szebenyi and Moffat (1986) for the crystalline state of Ca^{2+}-loaded minor A bovine calbindin D_{9k} and those identified in solution for intact porcine calbindin D_{9k}. There are, however, some minor differences relating to helices fraying open at their ends, a common observation for helices in solution (Chazin et al., 1988a). The sequence locations of helices I–III are essentially identical in the X-ray crystal structure and our solution studies. Two nonconservative substitutions at positions 4 and 8 and one conservative and two nonconservative substitutions in helix II (identified in Figure 3) have no apparent effect on backbone conformation. Helix IV extends only to Ser74 in solution. Furthermore, resonance line widths indicate that residue Ser74 (and Gln75) is significantly more flexible than the majority of the other residues, which implies that in solution the helix is fraying open at the C-terminus. The only significant difference between the bovine crystal and porcine solution structures is in the loop region connecting helix II and helix III. In solution there is no apparent secondary structure in this loop, whereas residues Pro37–Leu40 constitute a short turn of irregular helix in the crystal structure. This discrepancy may be related to cis–trans isomerism of Pro43 (Chazin et al., 1989).

The two Ca^{2+} binding loops in calbindin D_{9k} are clearly very different from each other. Only the C-terminal site II has the typical EF-hand structure with a 12-residue loop (Szebenyi & Moffat, 1986). Our previous ^{43}Ca and ^{113}Cd NMR studies of calbindin D_{9k} (Vogel et al., 1985) and studies of several mutant proteins (Linse et al., 1987) indicate that the two calcium binding sites provide markedly different environments for the metal ion. These structural differences contrast sharply with the similarity of the binding constants in the two sites and strongly suggest cooperative Ca^{2+} binding. Analysis of the macroscopic Ca^{2+} binding constants indicates binding cooperativity (Linse et al., 1987). Structural differences between the two Ca^{2+} binding loops are clearly detected in our 2D NMR studies. In loop I there is a very close approach between the backbone of the second and seventh residues, clearly evident from the strong NOESY cross peak between the C^α protons of Ala15 and Pro20. We estimate that these protons are separated by less than 3 Å. In loop II, there is no indication that any pairs of C^α protons are within 5 Å of each other. Ongoing studies to determine the complete three-dimensional structures of porcine and bovine calbindin D_{9k} should show if this close contact is the result of the extra length of the Ca^{2+} ion binding loop or the presence of a proline in the loop or both combined.

Acknowledgments

We thank Johan Kördel for helpful discussions concerning his independent 2D ^{1}H NMR analysis of recombinant bovine calbindin D_{9k}, Dr. Mark Rance for continued support with experimental methods, and Kathy Carpenter for assistance in the preparation of the manuscript. We also acknowledge Dr. Joseph Parello, Montpellier, for the communication of material prior to publication.

References

Billeter, M., Braun, W., & Wüthrich, K. (1982) *J. Mol. Biol. 155*, 321–346.

Brodin, P., Grundström, T., Hofmann, T., Drakenberg, T., Thulin, E., & Forsén, S. (1986) *Biochemistry 25*, 5371–5377.

Chazin, W. J., & Wright, P. E. (1987) *Biopolymers 26*, 973–977.

Chazin, W. J., Rance, M., & Wright, P. E. (1987) *FEBS Lett. 222*, 109–114.

Chazin, W. J., Hugli, T. E., & Wright, P. E. (1988a) *Biochemistry 27*, 9139–9148.

Chazin, W. J., Rance, M., & Wright, P. E. (1988b) *J. Mol. Biol. 202*, 603–626.

Chazin, W. J., Kördel, J., Drakenberg, T., Thulin, E., Brodin, P., Grundström, T., & Forsén, S. (1989) *Proc. Natl. Acad. Sci. U.S.A. 86*, 2195–2198.

Corradino, R. A., Fullmer, C. S., & Wasserman, R. H. (1976) *Arch. Biochem. Biophys. 174*, 738–742.

Dalgarno, D. C., Levine, B. A., Williams, R. J. P., Fullmer, C. S., & Wasserman, R. H. (1983) *Eur. J. Biochem. 137*, 523–529.

Davis, D. G. (1989) *J. Magn. Reson. 81*, 603–607.

Drescher, D., & De Luca, H. F. (1971) *Biochemistry 10*, 2302–2307.

Forsén, S., Linse, S., Thulin, E., Lindegård, B., Martin, S. R., Bayley, P. M., Brodin, P., & Grundström, T. (1988) *Eur. J. Biochem. 177*, 47–52.

Fullmer, C. S., & Wasserman, R. H. (1973) *Biochem. Biophys. Acta 317*, 172–186.

Fullmer, C. S., & Wasserman, R. H. (1981) *J. Biol. Chem. 256*, 5669–5671.

Hitchman, A. J. W., & Harrison, J. E. (1972) *Can. J. Biochem. 50*, 758–765.

Hitchman, A. J. W., Kerr, M. K., & Harrison, J. E. (1973) *Arch. Biochem. Biophys. 155*, 221–223.

Hofmann, T., Kawakami, M., Hitchmann, A. J. W., Harrison, J. E., & Dorrington, K. J. (1979) *Can. J. Biochem. 58*, 737–748.

Ikura, M., Minowa, O., Yazawa, M., Yagi, K., & Hikichi, K. (1987) *FEBS Lett. 219*, 17–21.

Kallfelz, F. A., Taylor, A. N., & Wasserman, R. H. (1986) *Proc. Soc. Exp. Biol. Med. 125*, 54–58.

Kördel, J., Forsen, S., & Chazin, W. J. (1989) *Biochemistry* (in press).

Kretsinger, R. H. (1972) *Nature (London), New Biol. 240*, 85.

Linse, S., Brodin, P., Drakenberg, T., Thulin, E., Sellers, P., Elmdén, K., Grundström, T., & Forsén, S. (1987) *Biochemistry 26*, 6723–6735.

Linse, S., Brodin, P., Johansson, C., Thulin, E., Grundström, T., & Forsén, S. (1988) *Nature (London) 335*, 651–652.

Mayel-Afshar, S., Lane, S. M., & Lawson, D. E. M. (1988) *J. Biol. Chem. 263*, 4355–4361.

Padilla, A., Cavé, A., & Parello, J. (1988) *J. Mol. Biol. 204*, 995–1017.

Szebenyi, D. M. E., & Moffat, K. (1986) *J. Biol. Chem. 261*, 8761–8776.

Taylor, A. N. (1983) in *Calcium Binding Proteins* (de Bernard, B., Sottocasa, G. L., Sandri, G., Carofoli, E., Taylor, A. N., Vanaman, T. C., & Williams, R. J. P., Eds.) pp 208–213, Elsevier/North-Holland, New York.

Tsuda, S., Hasegawa, Y., Yoshida, M., Yagi, K., & Hikichi, K. (1988) *Biochemistry 27*, 4120–4126.

Vogel, H. J., Drakenberg, T., Forsén, S., O'Neil, J. D. J., & Hofmann, T. (1985) *Biochemistry 24*, 3870–3876.

Wagner, G., Neuhaus, D., Wörgötter, E., Vašák, M., Kägi, J. H. R., & Wüthrich, K. (1986) *J. Mol. Biol. 187*, 131–135.

Wasserman, R. H., Shimara, F., Meyer, S. A., & Fullmer, C. S. (1983) in *Calcium Binding Proteins* (de Bernard, B.,

Sottocasa, G. L., Sandri, G., Carafoli, E., Taylor, A. N., Vanaman, T. C., & Williams, R. J. P., Eds.) pp 183-188, Elsevier/North-Holland, New York.
Wendt, B., Hofmann, T., Martin, S. R., Bayley, P. M., Brodin, P., Grundström, T., Thulin, E., Linse, S., & Forsén, S. (1988) *Eur. J. Biochem. 175*, 439-445.
Wüthrich, K. (1986) *NMR of Proteins and Nucleic Acids*, Wiley, New York.
Wüthrich, K., Billeter, M., & Braun, W. (1984) *J. Mol. Biol. 180*, 715-740.

Removal of the 9-Methyl Group of Retinal Inhibits Signal Transduction in the Visual Process. A Fourier Transform Infrared and Biochemical Investigation†

Ulrich M. Ganter,‡ Eduard D. Schmid,§ Dolores Perez-Sala,‖ Robert R. Rando,‖ and Friedrich Siebert*,‡

Institut für Biophysik und Strahlenbiologie and Institut für Physikalische Chemie, Albert-Ludwig-Universität Freiburg, Albertstrasse 23, D-7800 Freiburg im Breisgau, FRG, and Department of Biological Chemistry and Molecular Pharmacology, Harvard Medical School, 250 Longwood Avenue, Boston, Massachusetts 02115

Received September 13, 1988; Revised Manuscript Received February 14, 1989

ABSTRACT: The photoreaction of opsin regenerated with 9-demethylretinal has been investigated by UV-vis spectroscopy, flash photolysis experiments, and Fourier transform infrared difference spectroscopy. In addition, the capability of the illuminated pigment to activate the retinal G-protein has been tested. The photoproduct, which can be stabilized at 77 K, resembles more the lumirhodopsin species, and only minor further changes occur upon warming the sample to 170 K (stabilizing lumirhodopsin). UV-vis spectroscopy reveals no further changes at 240 K (stabilizing metarhodopsin I), but infrared difference spectroscopy shows that the protein as well as the chromophore undergoes further molecular changes which are, however, different from those observed for unmodified metarhodopsin I. UV-vis spectroscopy, flash photolysis experiments, and infrared difference spectroscopy demonstrate that an intermediate different from metarhodopsin II is produced at room temperature, of which the Schiff base is still protonated. The illuminated pigment was able to activate G-protein, as assayed by monitoring the exchange of GDP for GTPγS in purified G-protein, only to a very limited extent (approximately 8% as compared to rhodopsin). The results are interpreted in terms of a specific steric interaction of the 9-methyl group of the retinal in rhodopsin with the protein, which is required to initiate the molecular changes necessary for G-protein activation. The residual activation suggests a conformer of the photolyzed pigment which mimics metarhodopsin II to a very limited extent.

Rhodopsin, the visual pigment of vertebrate rods, consists of the protein opsin and the chromophore 11-*cis*-retinal (Wald, 1968) which is bound to lysine-296 (Ovchinnikov, 1983) by a protonated Schiff base linkage (Oseroff & Callender, 1974). Upon absorption of light, the chromophore is converted to the all-trans isomer already in the primary photoproduct (Palings et al., 1987; Bagley et al., 1985; Ganter et al., 1988), and, through a series of intermediates, rhodopsin decays to *all-trans*-retinal and opsin. One of these intermediates, metarhodopsin II, possesses a distinct conformation which enables it to activate an enzyme cascade which finally results in the change of the electric potential of the cell (Stryer, 1986). Because of the multitude of proline residues in rhodopsin and in a number of structural-related hormone receptors, Brandl and Deber (1986) suggested that the change in the conformation of rhodopsin which activates the enzyme cascade is caused by a cis-trans isomerization of a proline residue. However, little is known of how the retinal isomerization is linked to the structural changes occurring in metarhodopsin II.

Resonance Raman and Fourier transform infrared (FTIR)[1] difference spectroscopy provides information on molecular events during the photoreaction [e.g., see Palings et al. (1987), Bagley et al. (1985), and Ganter et al. (1988)]. Because FTIR spectroscopy covers spectral changes of both the chromophore and the surrounding proteins, this method is well-suited for observing chromophore-protein interactions. Previously, we have reported spectra on the rhodopsin-isorhodopsin and rhodopsin-bathorhodopsin (Siebert et al., 1983) and on the rhodopsin-lumirhodopsin transitions (Ganter et al., 1988). During the rhodopsin-lumirhodopsin transition, three carbonyl groups are altered, two of which could be assigned to protonated carboxylic acids and the other to the amide I vibration of an amino acid bound to the amino terminus of a proline residue. De Grip et al. (1985) reported on changes occurring during the rhodopsin-metarhodopsin I and the rhodopsin-metarhodopsin II transitions in the region of the carbonyl stretching vibrations. Rothschild et al. (1987) studied the alterations in the protein during the decay of the metarhodopsin II species.

Detailed molecular information on the visual pigment was obtained by regenerating opsin with synthetic retinal analogues. In a recent review, Derguini and Nakanishi (1986) described

† This work was supported by the Deutsche Forschungsgemeinschaft (Grant SFB 60-G-9, A-4) and by NIH Grant EY 03624. D.P.-S. is a recipient of a CSIC (Spain) postdoctoral fellowship.
* To whom correspondence should be addressed.
‡ Institut für Biophysik und Strahlembiologie.
§ Institut für Physikalische Chemie.
‖ Harvard Medical School.

[1] Abbreviations: FTIR, Fourier transform infrared spectroscopy; HOOP, hydrogen out of plane vibration; ROS, rod outer segment(s); 9-H, 9-demethyl; GDP, guanosine 5′-diphosphate; GTP, guanosine 5′-triphosphate; GTPγS, guanosine 5′-*O*-(3-thiotriphosphate).

0006-2960/89/0428-5954$01.50/0